

Supporting Information

Photoinduced ligand dissociation follows reverse energy gap law: nitrile photodissociation from low energy ³MLCT excited states

Lauren M. Loftus,[‡] Jeffrey J. Rack,[§] and Claudia Turro^{*‡}

[‡]*Department of Chemistry and Biochemistry, The Ohio State University, Columbus, OH 43210, USA*

[§]*Department of Chemistry and Chemical Biology, University of New Mexico, Albuquerque, NM 87131, USA*

Corresponding author: turro.1@osu.edu

Experimental Details

Materials. All complexes were synthesized according to literature procedures.^{S1,S2} CH₃CN for both fsTA and nsTA experiments was purified using an MBraun MB SPS-5 solvent purification system with alumina/molecular sieve-based columns or distilled over CaH₂.

Instrumentation. Steady-state electronic absorption spectra were collected using an Agilent Cary 8453 or 8454 diode array spectrophotometer in acetone or CH₃CN. Ultrafast transient absorption data for all complexes was collected on an upgraded homebuilt system; both systems have been previously described elsewhere.^{S3,S4} Nanosecond transient absorption data was collected using a basiScan tunable optical parametric oscillator (Spectra-Physics) pumped by a frequency-tripled Quanta-Ray INDI Nd:YAG laser (Spectra-Physics, ~6 ns pulses at 10 Hz), and an LP980 spectrometer system (Edinburgh Instruments) equipped with a 150 W Xe arc lamp as the white light probe. Spectral measurements were collected using an ICCD camera (iStar, Andor Technology) and single wavelength kinetic traces were collected using a PMT and digital oscilloscope (Tektronix MDO3022, 200 MHz, 2.5 GS/s).^{S5} The instrument response function (IRF) in CH₃CN was measured to be 12 ns (fwhm). Time-resolved infrared spectroscopy (TRIR) was performed on **8** using a previously described homebuilt system.^{S6} Briefly, a Ti:sapphire oscillator (Mantis, Coherent) is used to seed a high-energy Ti:sapphire regenerative amplifier (Legend HE USP, Coherent/Positive Light) to generate 40 fs pulses of 800 nm at 2.5 mJ and 1 kHz. The beam is then split to pump two OPAs (OPerA, Coherent); the first OPA is equipped with either a SFG or UV-Vis module to generate a pump pulse tunable from ~240 – 2600 nm, while the second OPA is equipped with a DFG module to generate mid-IR probe pulses that are tunable from 5000 – 1000 cm⁻¹. The probe pulse is then split into a reference and a probe beam using a Ge beamsplitter, and after passing through the sample both beams are spectrally dispersed by a Triax 320 spectrograph and imaged using a liquid N₂-cooled HgCdTe detector (2 x 32 pixels, InfraRed Associates, Inc.) with ~4 cm⁻¹ resolution. A home-developed LabView program was used to collect the spectral data, and the IRF is ~300 fs (fwhm).

Methods. Ultrafast transient absorption experiments were collected using a CaF₂ flow cell with a path length of 1 mm. Samples were prepared to have an absorbance of 0.5 at the indicated excitation wavelength in CH₃CN, and the power of the pump laser was set to 2.5 μJ at the sample. The electronic absorption spectrum of the sample was measured before and after the fsTA experiment to ensure no sample degradation had occurred. The polarization angle between the pump and probe beams was set to the magic angle (54.7°) to avoid effects from rotational diffusion. Measurements were repeated three times at each time delay and averaged, and the spectra were corrected for the chirp in the white light continuum.^{S7} Single wavelength kinetic traces were fit to mono- or biexponential decays as needed using the Igor Pro software package (version 8.03, WaveMetrics).^{S8}

Nanosecond transient absorption data was collected using a 1x1 cm quartz cuvette, and all samples were sparged with N₂ for 20 min. prior to measurement to remove dissolved O₂ from the sample. Samples were prepared to have an absorbance of 0.5 at the indicated excitation wavelength in CH₃CN, and the power of the pump laser was set between 5 – 7 mJ. The electronic absorption spectrum of each sample was measured before and after the nsTA experiment to ensure no sample degradation had occurred. Due to their relatively short lifetimes, the kinetic traces were fit to a single decay component using a reconvolution fit in the L900 software program (Edinburgh Instruments) that incorporated the measured instrument response function of 12 ns (fwhm).

Time-resolved infrared spectra for **8** were collected at room temperature in a semi-demountable Perkin-Elmer IR cell. The sample was prepared in CD₃CN to have an IR transmittance of ~30% in the region of interest and was sealed between two 4 mm thick CaF₂ plates separated by a 0.1 mm Teflon spacer, and was excited using 518 nm light (2 μJ at the sample). The infrared spectrum of the sample was measured before and after the experiment to ensure no sample degradation had occurred. The spectra shown are an average of two sets of data, and single wavelength kinetic traces were fit to mono- or biexponential decays as needed in Igor Pro.^{S8}

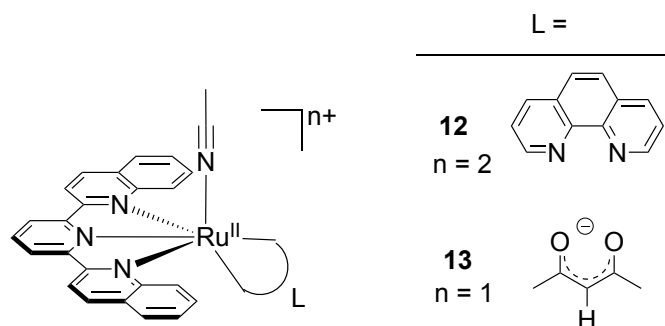


Figure S1. Molecular structures of complexes **12** and **13**.

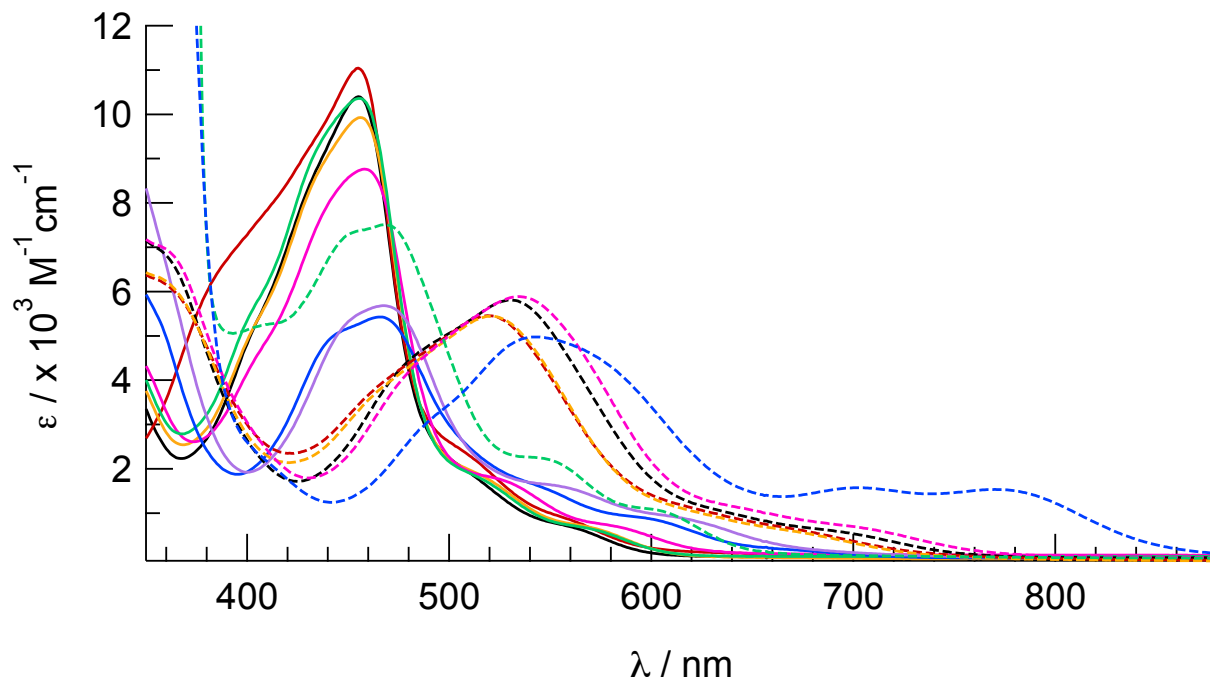


Figure S2. Electronic absorption spectra in acetone for **1** (black), **2** (red), **3** (orange), **4** (pink), **5** (green), **6** (blue), **7** (purple), **8** (dashed black), **9** (dashed red), **10** (dashed orange), **11** (dashed pink), **12** (dashed green), and **13** (dashed blue).

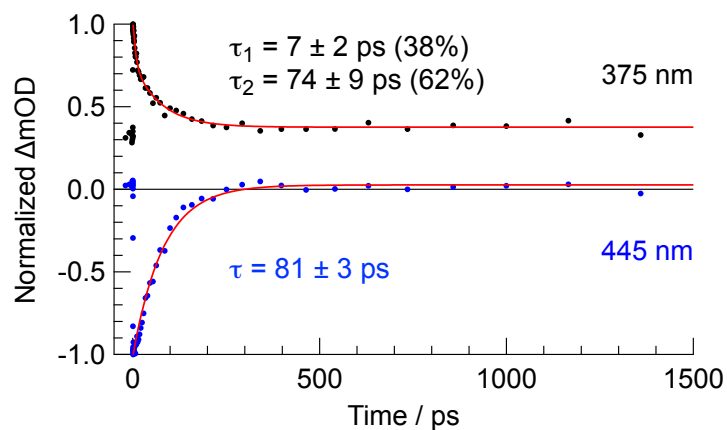


Figure S3. Normalized representative fsTA single wavelength kinetic traces and fits from the excited state absorption (375 nm) and ground state bleach (445 nm) regions of **1**.

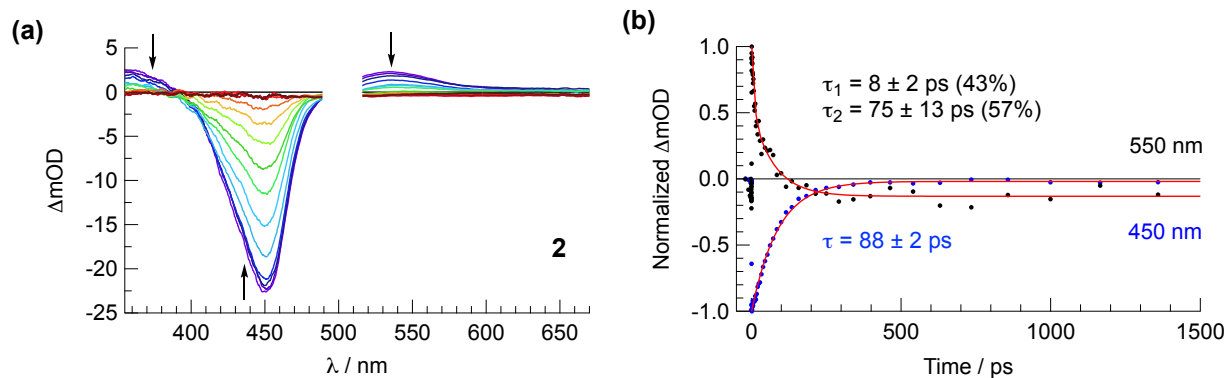


Figure S4. (a) fsTA spectra in CH_3CN for **2** collected at 1, 3, 5, 9, 21, 39, 62, 85, 116, 158, 215, 397, 630, 999 and 2928 ps after the laser pulse ($\lambda_{\text{ex}} = 505$ nm, fwhm ~ 85 fs, baseline collected at -20 ps). (b) Normalized representative single wavelength kinetic traces and fits from the excited state absorption (550 nm) and ground state bleach (450 nm) regions of **2**.

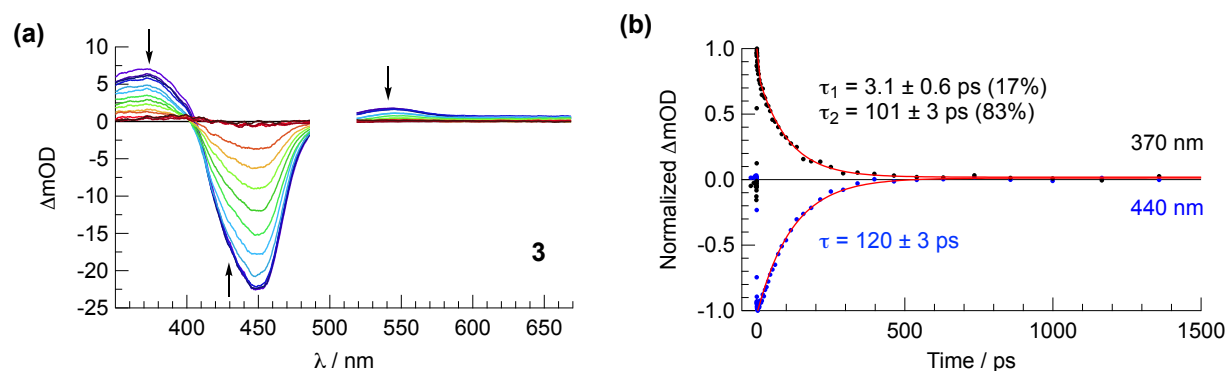


Figure S5. (a) fsTA spectra in CH_3CN for **3** collected at 1, 3, 6, 9, 24, 39, 62, 85, 115, 157, 214, 397, 630, 999 and 2928 ps after the laser pulse ($\lambda_{\text{ex}} = 505$ nm, fwhm ~ 85 fs, baseline collected at -20 ps). (b) Normalized representative single wavelength kinetic traces and fits from the excited state absorption (370 nm) and ground state bleach (440 nm) regions of **3**.

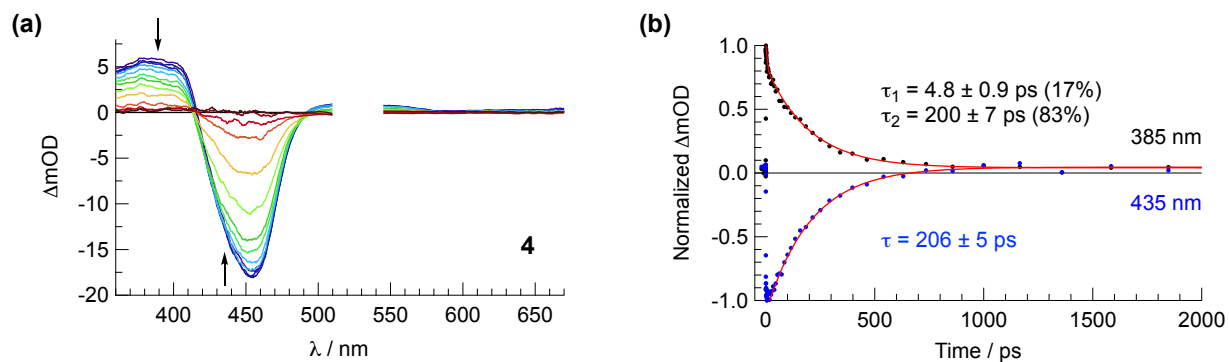


Figure S6. (a) fsTA spectra in CH₃CN for **4** collected at 1, 3, 6, 9, 21, 46, 62, 116, 215, 397, 630, 999 and 2928 ps after the laser pulse ($\lambda_{\text{ex}} = 530$ nm, fwhm ~ 85 fs, baseline collected at -20 ps). (b) Normalized representative single wavelength kinetic traces and fits from the excited state absorption (385 nm) and ground state bleach (435 nm) regions of **4**.

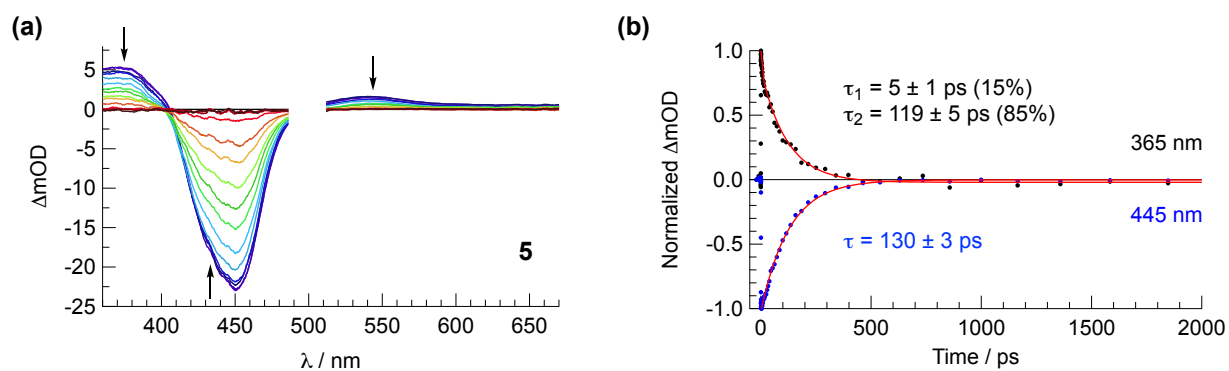


Figure S7. (a) fsTA spectra in CH₃CN for **5** collected at 1, 3, 6, 9, 20, 39, 62, 85, 115, 157, 214, 397, 630, 999 and 2928 ps after the laser pulse ($\lambda_{\text{ex}} = 505$ nm, fwhm ~ 85 fs, baseline collected at -20 ps). (b) Normalized representative single wavelength kinetic traces and fits from the excited state absorption (365 nm) and ground state bleach (445 nm) regions of **5**.

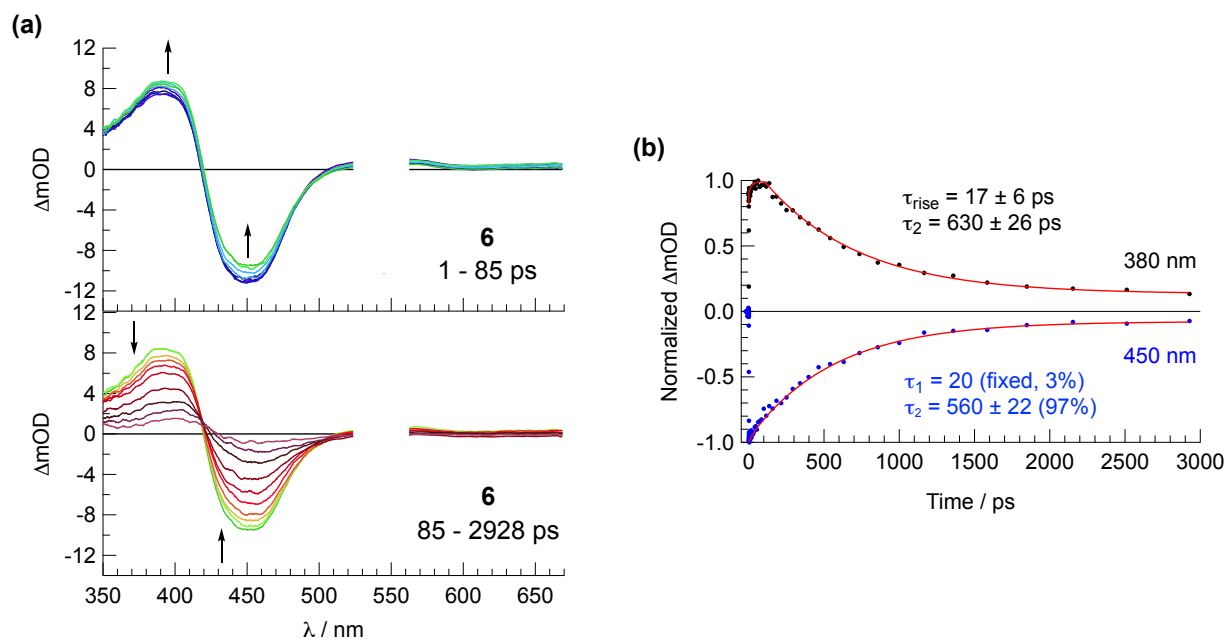


Figure S8. (a) fsTA spectra in CH_3CN for **6** collected at 1, 3, 7, 9, 21, 39, 62, 85, 116, 158, 215, 292, 397, 630, 999, 1584 and 2928 ps after the laser pulse ($\lambda_{\text{ex}} = 550$ nm, fwhm ~ 85 fs, baseline collected at -20 ps). (b) Normalized representative single wavelength kinetic traces and fits from the excited state absorption (380 nm) and ground state bleach (450 nm) regions of **6**.

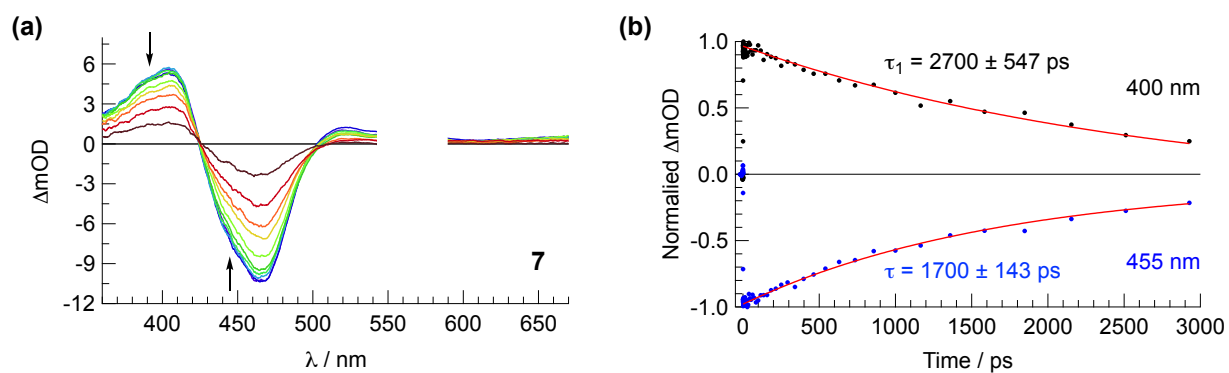


Figure S9. (a) fsTA spectra in CH_3CN for **7** collected at 1, 9, 21, 116, 215, 397, 630, 999, 1847 and 2928 ps after the laser pulse ($\lambda_{\text{ex}} = 565$ nm, fwhm ~ 85 fs, baseline collected at -20 ps). (b) Normalized representative single wavelength kinetic traces and fits from the excited state absorption (400 nm) and ground state bleach (455 nm) regions of **7**.

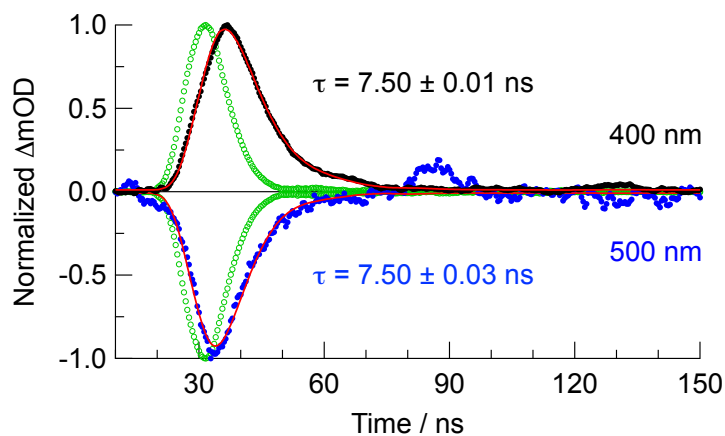


Figure S10. Normalized representative single wavelength kinetic traces and fits from the excited state absorption (400 nm) and ground state bleach (500 nm) regions of **8** ($\lambda_{\text{ex}} = 580$ nm, fwhm ~ 12 ns). The IRF is shown in hollow green circles.

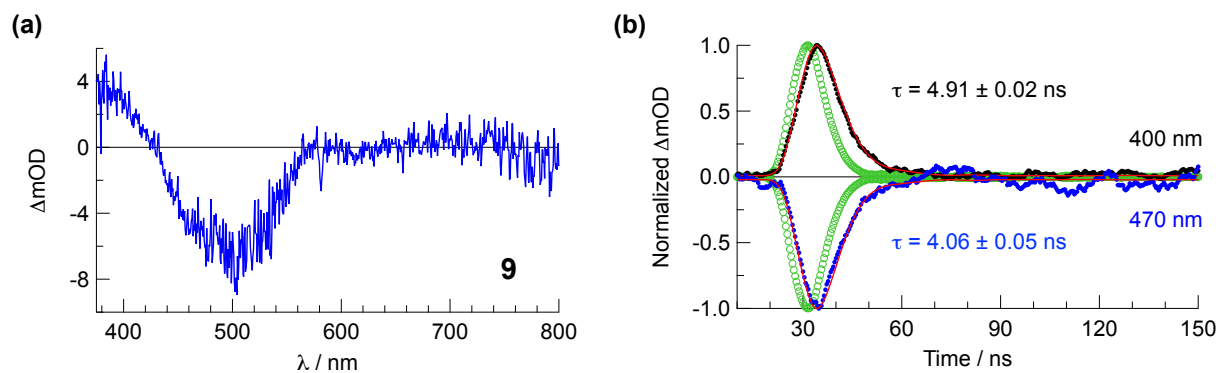


Figure S11. (a) nsTA spectrum in CH_3CN for **9** collected immediately following the laser pulse ($\lambda_{\text{ex}} = 580$ nm, fwhm ~ 12 ns). (b) Normalized representative single wavelength kinetic traces and fits from the excited state absorption (400 nm) and ground state bleach (470 nm) regions of **9**. The IRF is shown in hollow green circles.

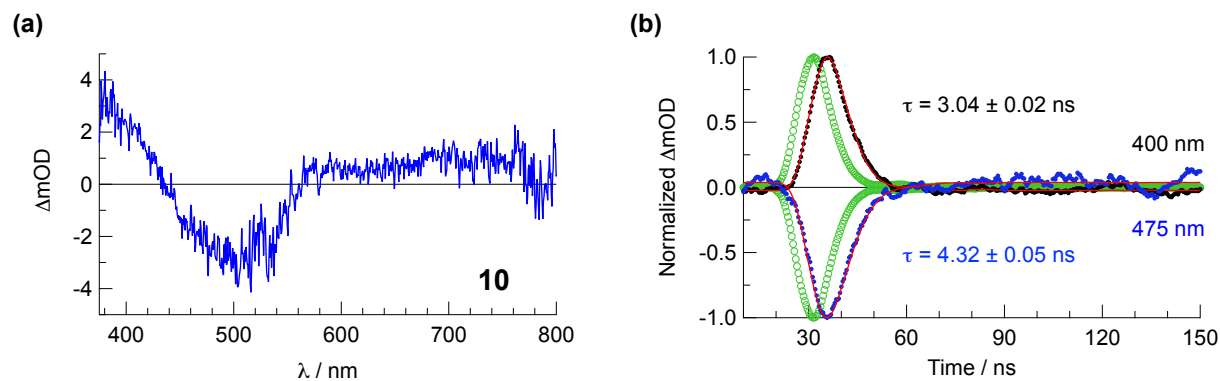


Figure S12. (a) nsTA spectrum in CH_3CN for **10** collected immediately following the laser pulse ($\lambda_{ex} = 580$ nm, fwhm ~ 12 ns). (b) Normalized representative single wavelength kinetic traces and fits from the excited state absorption (400 nm) and ground state bleach (475 nm) regions of **10**. The IRF is shown in hollow green circles.

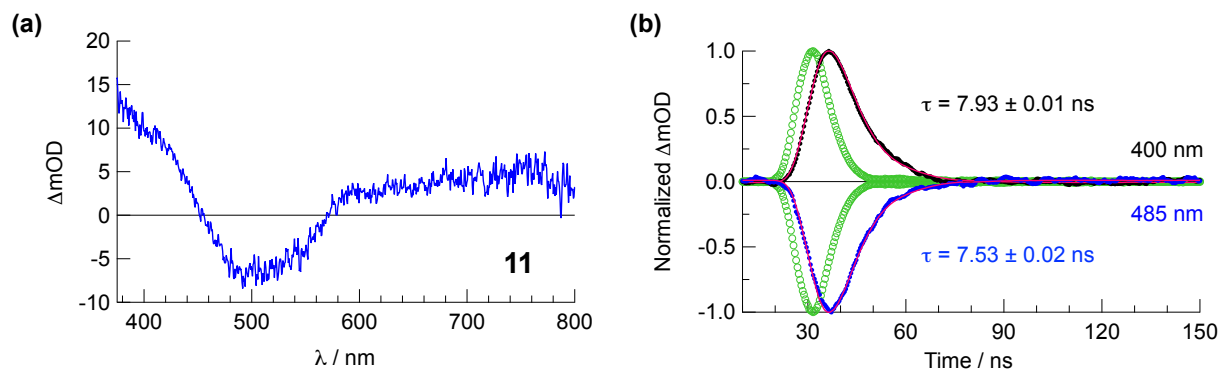


Figure S13. (a) nsTA spectrum in CH_3CN for **11** collected immediately following the laser pulse ($\lambda_{ex} = 580$ nm, fwhm ~ 12 ns). (b) Normalized representative single wavelength kinetic traces and fits from the excited state absorption (400 nm) and ground state bleach (485 nm) regions of **11**. The IRF is shown in hollow green circles.

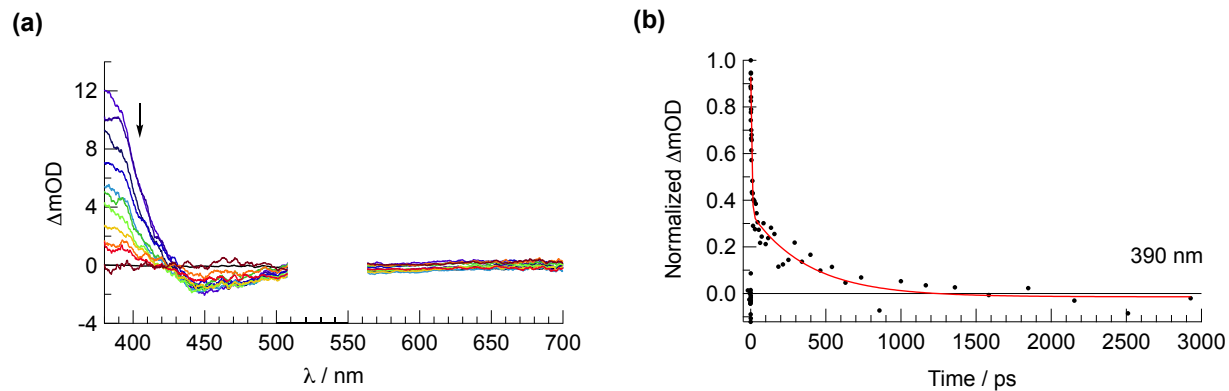


Figure S14. (a) fsTA of **12** in CH₃CN collected at 0.8, 1, 3, 4, 7, 17, 45, 99, 184, 463 and 1584 ps after the laser pulse ($\lambda_{\text{ex}} = 530$ nm, fwhm ~ 85 fs, baseline collected at -5 ps). (b) Normalized representative single wavelength kinetic trace and fit from the excited state absorption (390 nm) region of **12**.

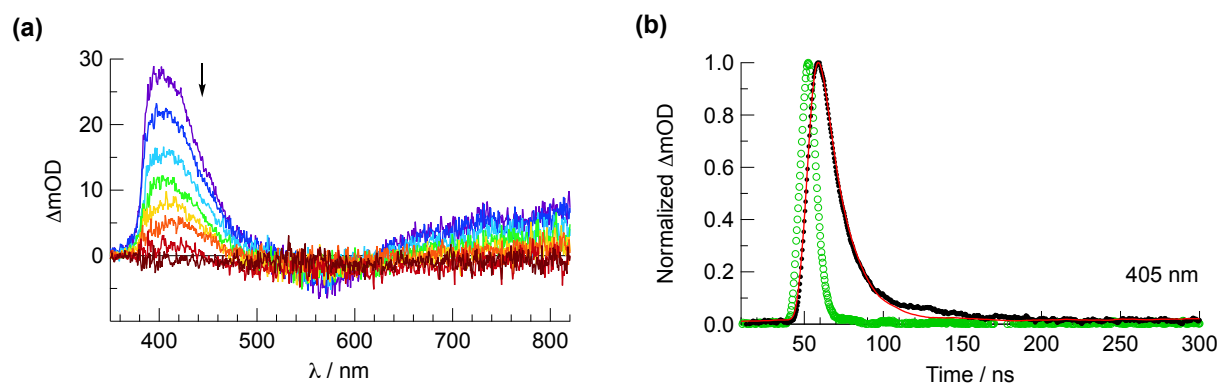


Figure S15. (a) nsTA spectrum in CH₃CN for **13** collected at 0, 5, 10, 15, 20, 35, 50 and 195 ns after the laser pulse ($\lambda_{\text{ex}} = 650$ nm, fwhm ~ 12 ns). (b) Normalized representative single wavelength kinetic trace and fit from the excited state absorption (405 nm) region of **13**. The IRF is shown in hollow green circles.

Table S1. Single wavelength kinetic fitting results for **1 – 11** from fsTA and nsTA spectroscopy at room temperature in CH₃CN.^a

Complex	ESA ($\pi \rightarrow \pi^*$) τ / ps ($\pm \sigma$)	Ground State Bleach τ / ps ($\pm \sigma$)	ESA (LMCT)^b τ / ps ($\pm \sigma$)	Averaged ³MLCT Lifetime^c τ / ps ($\pm \sigma$)
1	$\tau_1 = 6 \pm 1$ (40%) $\tau_2 = 75 \pm 11$ (60%)	$\tau_1 = \text{NA}^d$ $\tau_2 = 75 \pm 8$	$\tau_1 = 7 \pm 5$ (25%) $\tau_2 = 73 \pm 16$ (75%)	74 ± 9
2	$\tau_1 = 7 \pm 2$ (48%) $\tau_2 = 94 \pm 30$ (52%)	$\tau_1 = \text{NA}^d$ $\tau_2 = 86 \pm 3$	$\tau_1 = 8 \pm 2$ (43%) $\tau_2 = 73 \pm 12$ (57%)	84 ± 10
3	$\tau_1 = 4 \pm 1$ (22%) $\tau_2 = 99 \pm 8$ (78%)	$\tau_1 = \text{NA}^d$ $\tau_2 = 121 \pm 5$	$\tau_1 = 9 \pm 5$ (27%) $\tau_2 = 88 \pm 17$ (73%)	103 ± 20
4	$\tau_1 = 5.7 \pm 0.9$ (20%) $\tau_2 = 200 \pm 10$ (80%)	$\tau_1 = \text{NA}^d$ $\tau_2 = 210 \pm 10$		205 ± 10
5	$\tau_1 = 6 \pm 2$ (16%) $\tau_2 = 117 \pm 5$ (84%)	$\tau_1 = \text{NA}^d$ $\tau_2 = 125 \pm 4$	$\tau_1 = 11 \pm 6$ (29%) $\tau_2 = 117 \pm 23$ (71%)	120 ± 4
6	$\tau_1 = 20 \pm 8$ (rise) $\tau_2 = 650 \pm 30$	$\tau_1 = 20$ (fixed, 3%) $\tau_2 = 590 \pm 30$ (97%)		620 ± 50
7	2700 ± 600	1700 ± 200		2200 ± 600
8^e	7200 ± 300	6900 ± 500		7100 ± 400
9^e	4000 ± 1000	4600 ± 800		4400 ± 900
10^e	3500 ± 700	3800 ± 600		3700 ± 600
11^e	7800 ± 300	7900 ± 300		7800 ± 300

^a Values are reported as the average of single wavelength kinetic traces collected every 10 nm over the indicated feature. ^b Only complexes with sufficient signal-to-noise in this region were fit. ^c The overall ³MLCT excited state lifetime averages fitting results from both the excited state absorption and ground state bleach features of the complex, as the results suggest these features decay with the same time component in these complexes. These averaged lifetimes are the data points used in Fig. 4 of the main text. ^d Component not present. ^e Excited state lifetime from nsTA.

References

- S1. L. M. Loftus, K. F. Al-Afyouni, T. N. Rohrabough Jr., J. C. Gallucci, C. E. Moore, J. J. Rack and C. Turro, *J. Phys. Chem. C*, 2019, **123**, 10291-10299.
- S2. M. H. Al-Afyouni, T. N. Rohrabough Jr, K. F. Al-Afyouni and C. Turro, *Chem. Sci.*, 2018, **9**, 6711-6720.
- S3. G. Burdzinski, J. C. Hackett, J. Wang, T. L. Gustafson, C. M. Hadad and M. S. Platz, *J. Am. Chem. Soc.*, 2006, **128**, 13402-13411.
- S4. L. M. Loftus, A. Li, K. L. Fillman, P. D. Martin, J. J. Kodanko and C. Turro, *J. Am. Chem. Soc.*, 2017, **139**, 18295-18306.
- S5. T. N. Rohrabough Jr, K. A. Collins, C. Xue, J. K. White, J. J. Kodanko and C. Turro, *Dalton Trans.*, 2018, **47**, 11851-11858.
- S6. J. Wang, G. Burdzinski, J. Kubicki and M. S. Platz, *J. Am. Chem. Soc.*, 2008, **130**, 11195-11209.
- S7. T. Nakayama, Y. Amijima, K. Ibuki and K. Hamanoue, *Rev. Sci. Instrum.*, 1997, **68**, 4364-4371.
- S8. in *Fluorescence Lifetime Spectroscopy and Imaging: Principles and Applications in Biomedical Diagnostics*, eds. L. Marcu, P. M. W. French and D. S. Elson, CRC Press, Boca Raton, FL, USA, 1st edn., 2014.